Gyrokinetic simulations of ETG turbulence and zonal flows in positive/reversed shear tokamaks

Yasuhiro Idomura
Japan Atomic Energy Research Institute

Festival de Theorie 2005
Aix-en-Provance, France, 4-22 July 2005

Outline

- **Gyrokinetic simulations of toroidal ETG turbulence**
  - **Linear and quasi-linear analysis of ETG mode**
  - **ETG turbulence simulation in PS/RS tokamaks**
- **Self-organization in ETG turbulence**

Motivation to study ETG turbulence

- ETG turbulence is experimentally relevant candidate of χ_e in tokamak
  - High suppression threshold $\omega_{ExB} > \gamma$ than TEM (Stallard 1999)
  - Stiff T_e profile consistent with critical L_{te} of ETG (Hoang 2001)
- Issues to be addressed

  Does ρ_e scale ETG turbulence cause experimentaly relevant χ_e?
  - Yes: $\chi_e \sim 10 \chi_{GB}$ ($\chi_{GB}=v_{te}\,\rho_{te}^2/L_{te}$) in $\rho^{*-1}\sim\infty$ ($\rho^{*-1}=a/\rho_{te}$) local flux tube toroidal GK code (Jenko 2002)
  - No: $\chi_e \sim \chi_{GB}$ in $\rho^{*-1}\sim 100$ global toroidal GF code (Labit 2003)

  What kind of structure formations does ETG turbulence show?
  - Streamers: positive shear flux tube toroidal GK code (Jenko 2002)
  - Zonal flows: reversed shear global slab GK code (Idomura 2000)
- To examine these qualitatively and quantitatively different results, ETG turbulence is studied using global toroidal GK simulations
  - ρ^*-dependence of toroidal ETG modes
  - Zonal flow and streamer formations in PS/RS-ETG turbulence

Basic equations

- Electrostatic gyrokinetic equation (Hahm 1988)

$$H = \frac{1}{2} m_e v_{//}^2 + \mu B + q_e \langle \phi \rangle_g$$

$$\frac{DF_e}{Dt} = \frac{\partial F_e}{\partial t} + \{F_e, H\} = 0$$

$$\frac{d\mathbf{R}}{dt} \equiv \{\mathbf{R}, H\} = v_{//}\mathbf{b} + \frac{c}{q_e B_{//}^*}\mathbf{b} \times \left(q_e \nabla_{\mathbf{R}} \langle \phi \rangle_g + m_e v_{//}^2 \mathbf{b} \cdot \nabla_{\mathbf{R}} \mathbf{b} + \mu B \nabla_{\mathbf{R}} \ln B \right)$$

$$\frac{dv_{//}}{dt} \equiv \{v_{//}, H\} = -\frac{\mathbf{B}^*}{m_e B_{//}^*} \cdot \left(q_e \nabla_{\mathbf{R}} \langle \phi \rangle_g + m_e v_{//}^2 \mathbf{b} \cdot \nabla_{\mathbf{R}} \mathbf{b} + \mu B \nabla_{\mathbf{R}} \ln B \right)$$

$$\mathbf{B}^* = \mathbf{B} + \frac{c m_e v_{//}}{q_e} \nabla_{\mathbf{R}} \times \mathbf{b}, \quad \mu = \frac{m_e v_\perp^2}{2B}$$

- Gyrokinetic Poisson equation

$$-\nabla^2 \phi - \nabla_\perp \cdot \frac{\rho_{te}^2}{\lambda_{De}^2} \nabla_\perp \phi + \frac{1}{\lambda_{Di}^2} \phi = 4\pi q_e \int \delta F_e \delta\left([\mathbf{R} + \boldsymbol{\rho}_e] - \mathbf{x} \right) m_e^2 B_{//}^* d^6 \mathbf{Z}$$

Calculation models of ETG turbulence simulation

- Electrostatic GK toroidal PIC code
- Gyrokinetic electrons with adiabatic ions ($k_\perp \rho_{ti}$>>1)
- Annular wedge torus geometry
  - fixed B.C. $\phi = 0$
  - n = 0, N, 2N… (N=25~100)
- Quasi-ballooning representation
- Global profile effects (n_e, T_e, q, 1/r)
  - Self-consistent T_e, n_e are relaxed by heat/particle transport
  - ω^*_{te}-shearing effect
  - Reversed $q(r)$ profile
- Optimized particle loading
  - energy/particle conservation

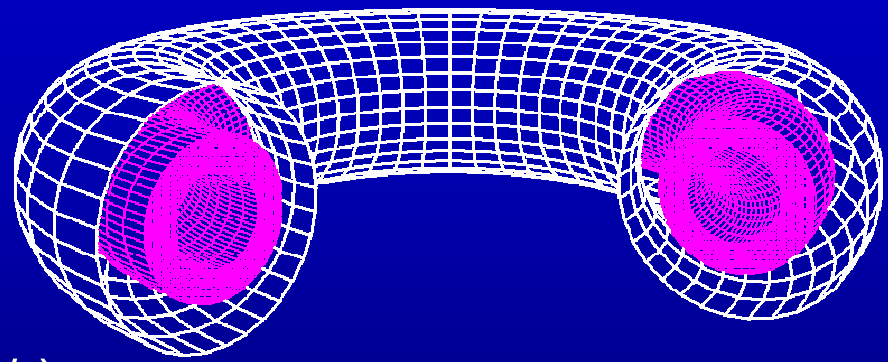

Validity of simulation is checked by conservation properties !

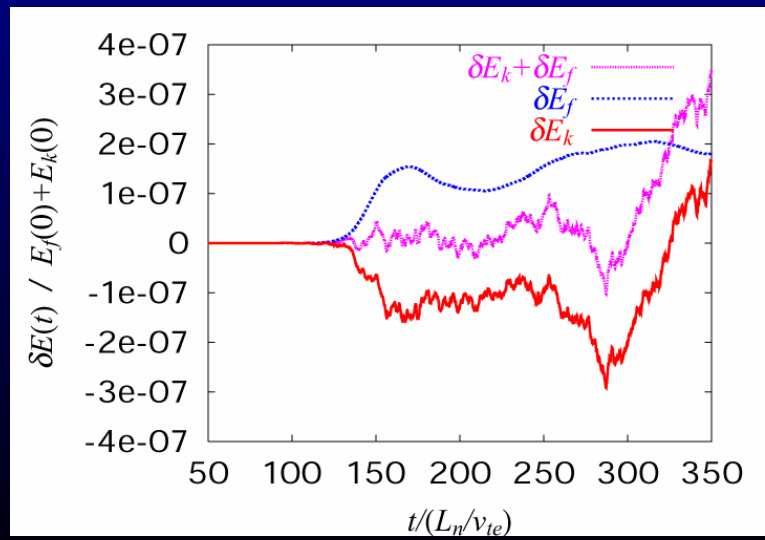

High-*n* solver with quasi-ballooning representation

$$\phi(r,\theta,\varphi)=\sum_n \hat{\phi}_n(r,\theta)e^{-in\varphi+in\hat{q}(r_s)\hat{\theta}},\quad \hat{\phi}_n(r,0)=\hat{\phi}_n(r,2\pi)e^{i2\pi n\hat{q}(r_s)},\quad r_s:\text{reference surface}$$

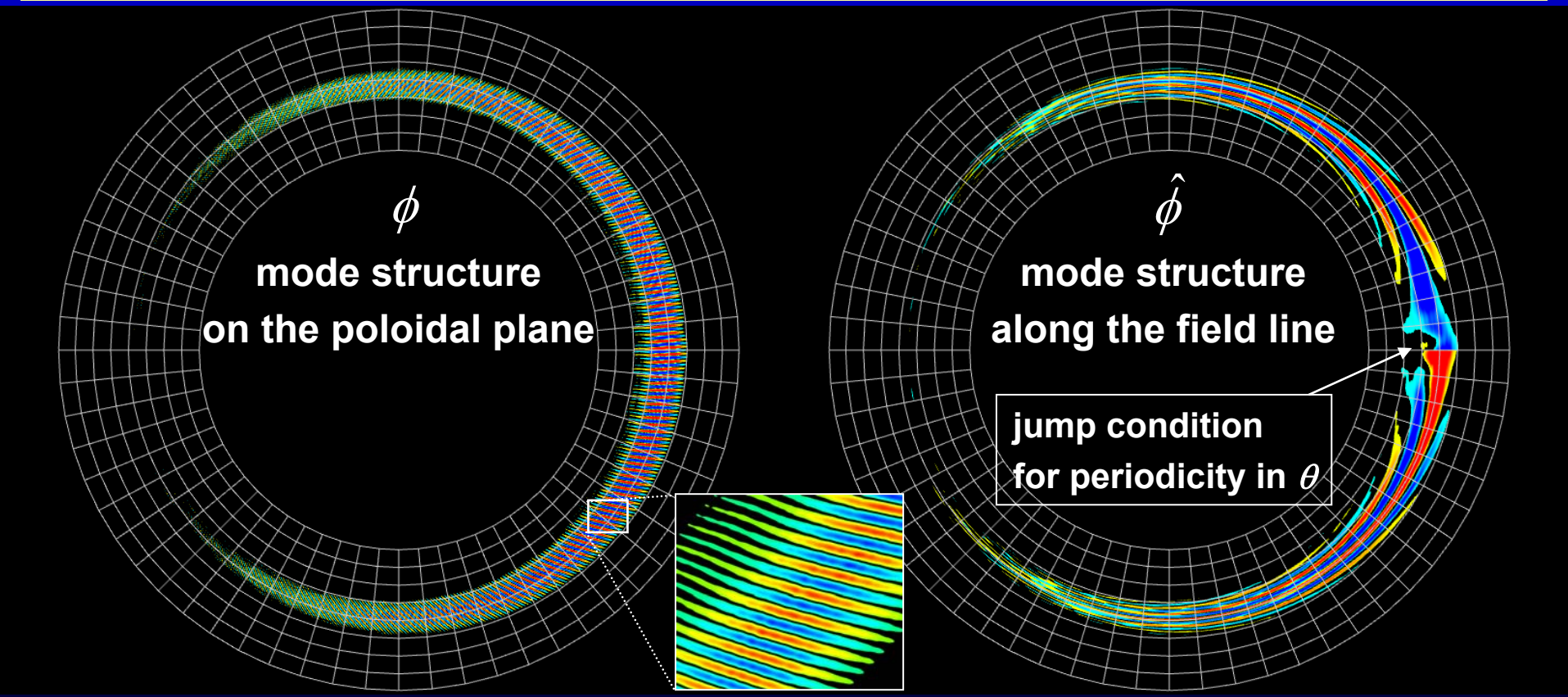

Realistic tokamak size $a/\rho_{te}\sim10^4$: $k_\theta\rho_{te}\sim1$ (q=1.4) ⟶ m=5000

- ~10^4 poloidal grids are needed without QB representation
- ~10^2 poloidal grids are enough with QB representation

Linear and quasi-linear analysis of ETG mode

Linear ETG growth rate spectrum

Cyclone like parameters (R_0/L_{te}=6.9, η_e=3.12, a~8600ρ_{te}~150ρ_{ti})

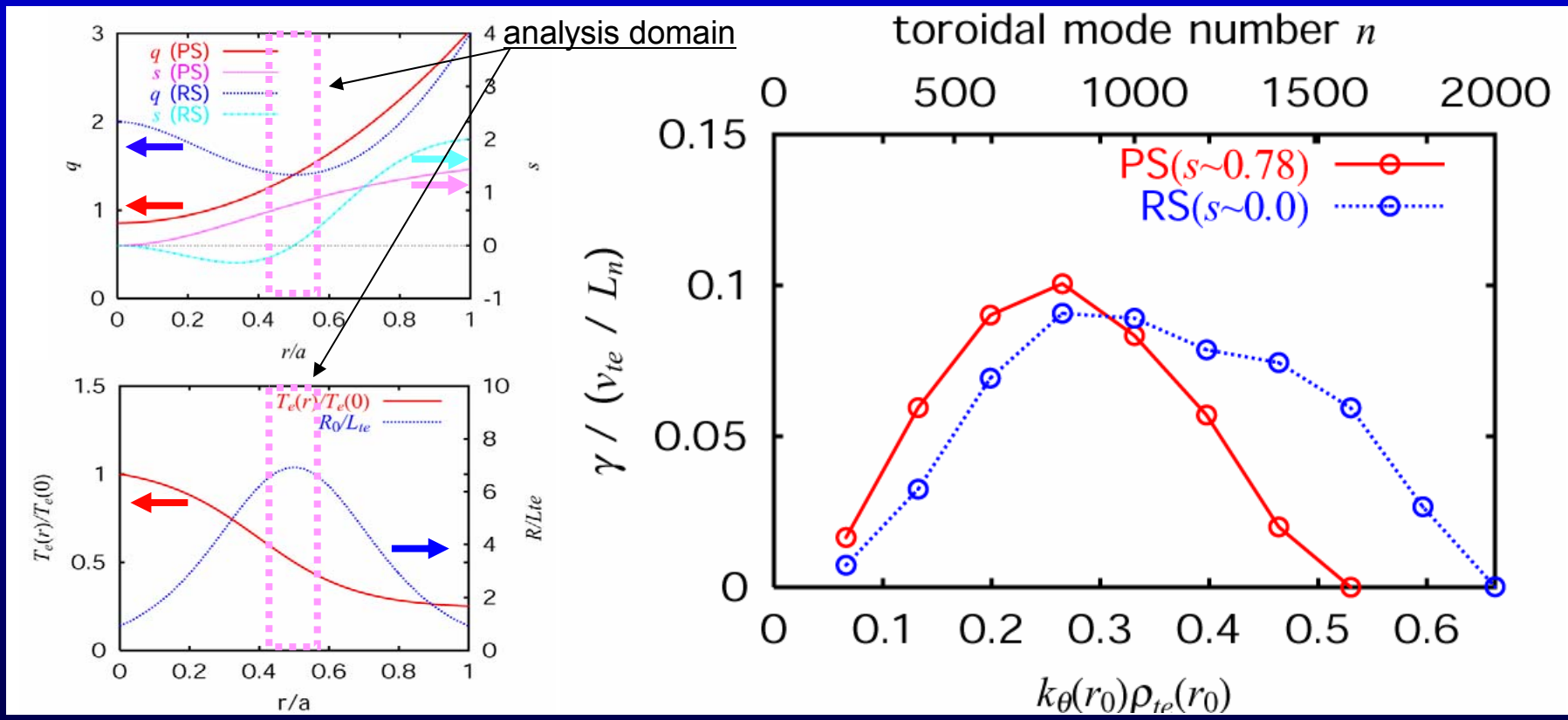

- Unstable region spreads over n~2000 (m~3000, $k_\theta\rho_{te}$~0.7)
- RS-ETG mode is excited around q_{min} surface (Idomura 2000)
- Almost the same γ_{max} in PS and RS configurations

Toroidal mode coupling in PS/RS configurations

- Positive shear configuration
- Reversed shear configuration

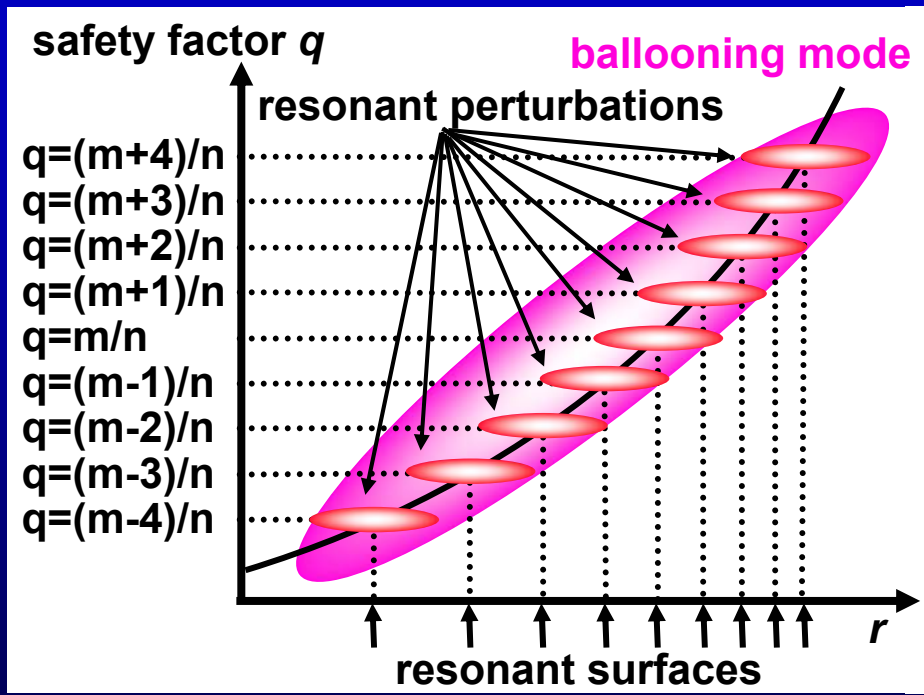

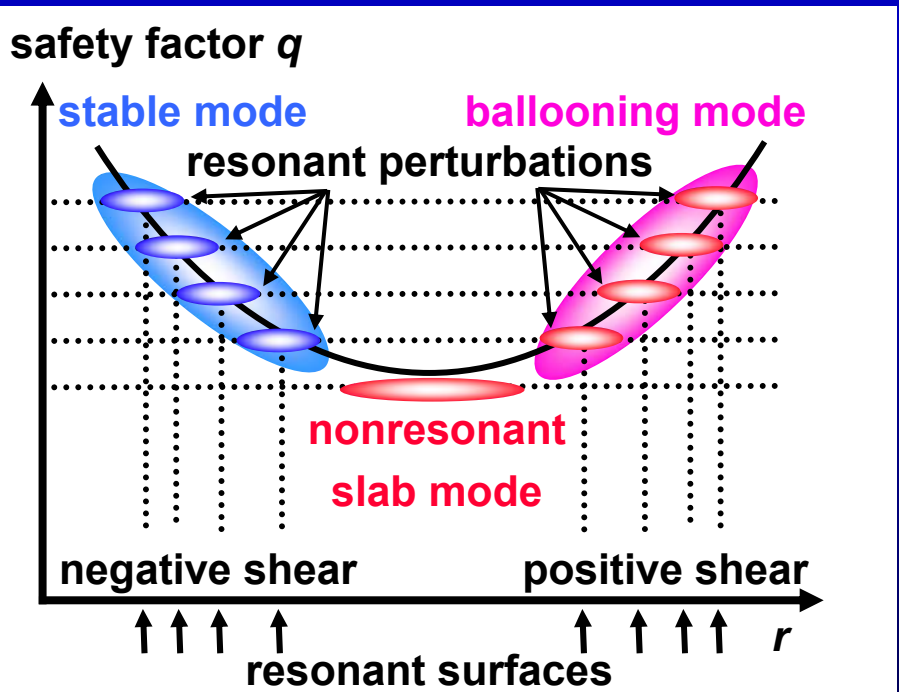

- Ballooning PS-ETG mode
- Big streamer structure in weak field side

- Slab like RS-ETG mode
- Single helicity feature in weak shear region

ρ^* scan of eigenfunctions in PS/RS tokamaks

- Positive shear configuration
- Reversed shear configuration

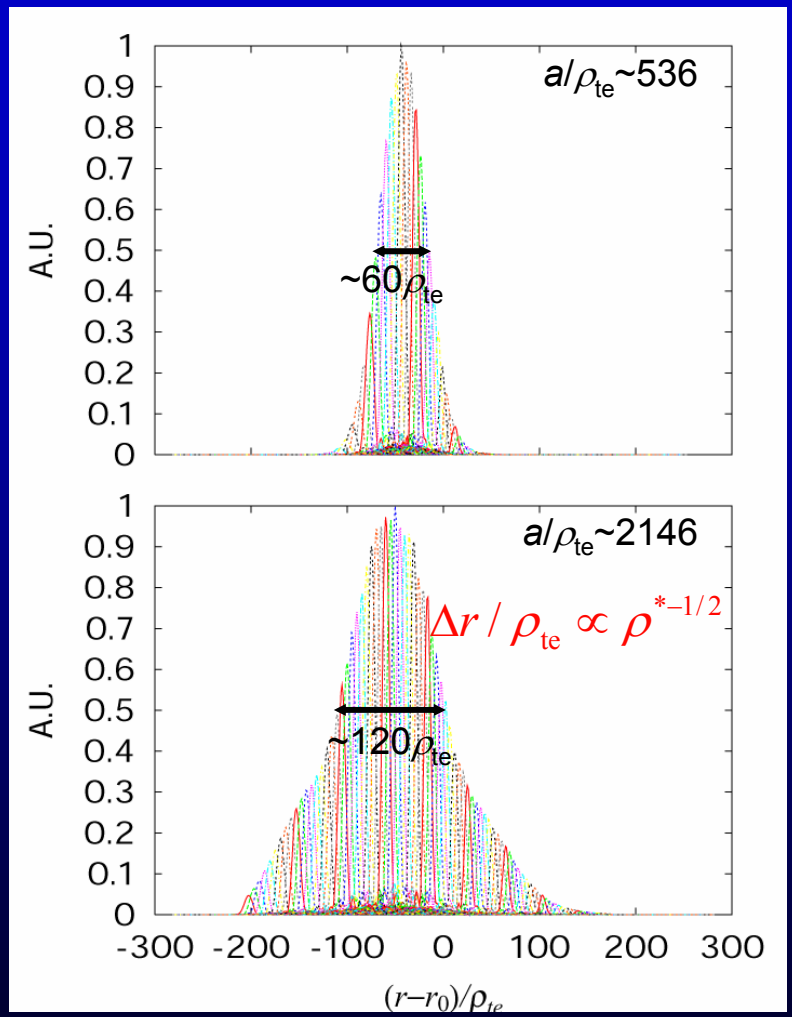

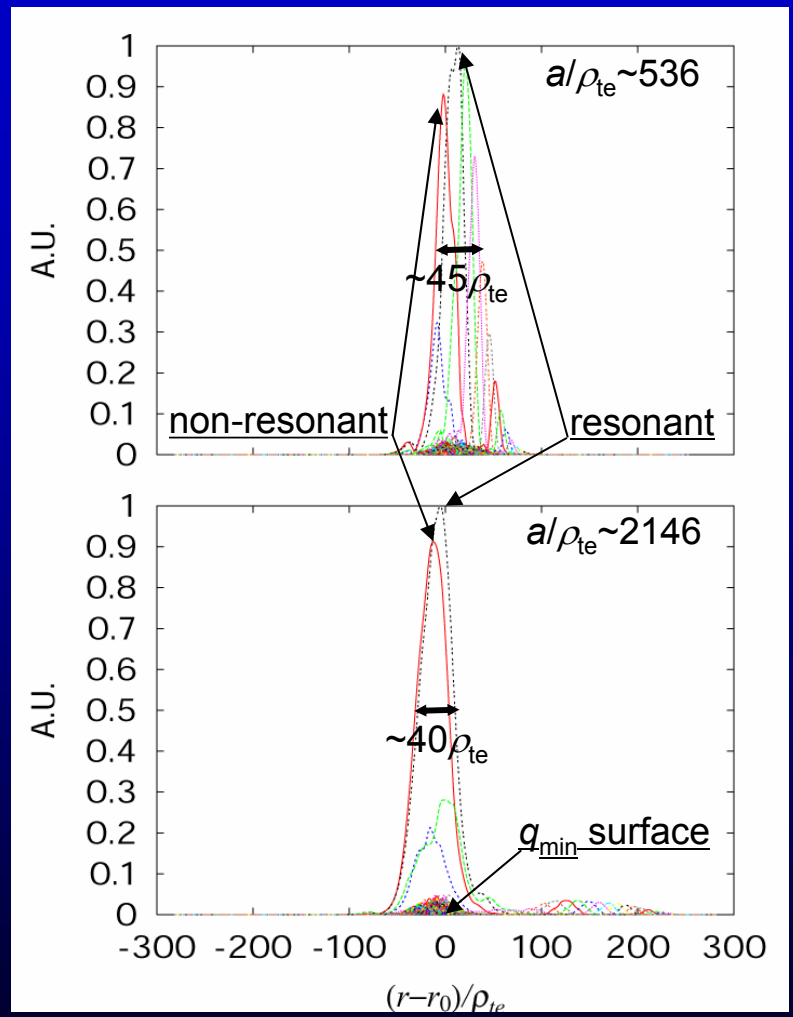

- Δr of PS-ETG mode is limited by ω^*-shearing effect (Kim 1994)
- Δr of RS-ETG mode is determined by q profile (Idomura 2000)

Mixing length theory and ρ^*-scaling

- Mixing length theory of ETG modes in PS/RS plasmas
  - PS-ETG mode $\Delta r / \rho_{te} \propto \rho^{*-1/2} \longrightarrow \chi_{ML} / \chi_{GB} \propto \gamma_n \rho^{*-1}$
  - RS-ETG mode $\Delta r / \rho_{te} \propto (L_{ns} / L_n)^{-1/2} \longrightarrow \chi_{ML} / \chi_{GB} \propto \gamma_n L_{ns} / L_n$

$$\gamma_n = \gamma L_n / v_{te} \qquad L_n = (d \ln n_e / dr)^{-1} \qquad L_{ns} = (2qR_0 / q''r)^{1/2}$$

- ρ^* scan of the saturation amplitude in single-*n* simulations

Fixed local parameters
R_0/L_{te}=6.9, η_e=3.12
$k_\theta \rho_{te}$~0.3, a/R_0=0.358
γ_{NL}: eddy turn over time

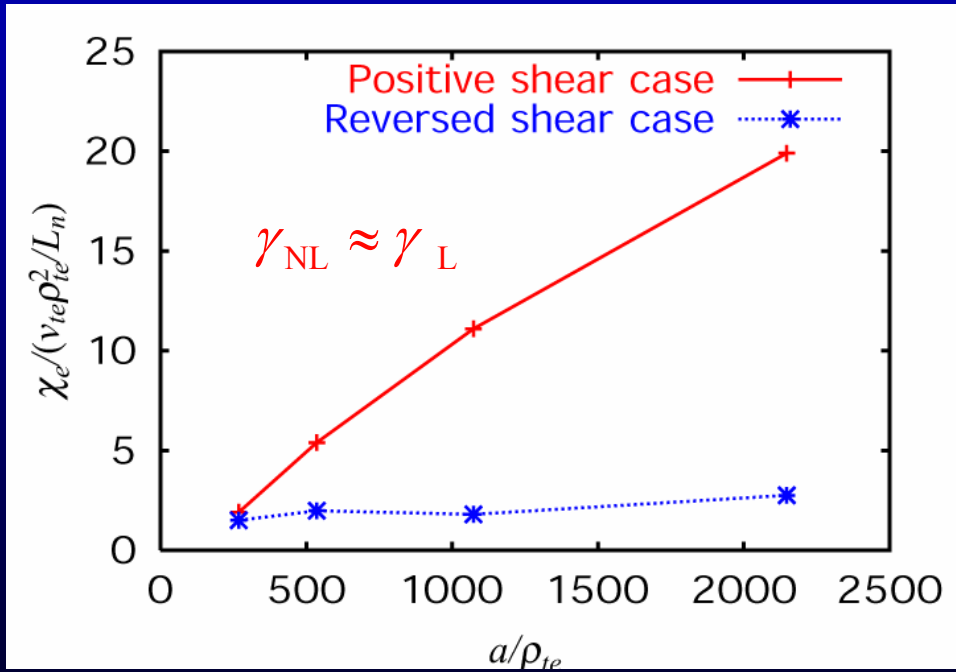

  - Small ρ^* PS-ETG modes give order of magnitude higher saturation level than RS-ETG and large ρ^* PS-ETG modes

ETG turbulence simulation in PS/RS tokamaks

Streamer formation in PS-ETG turbulence

- Linear phase ($t\, v_{te}/L_n$ ~110)

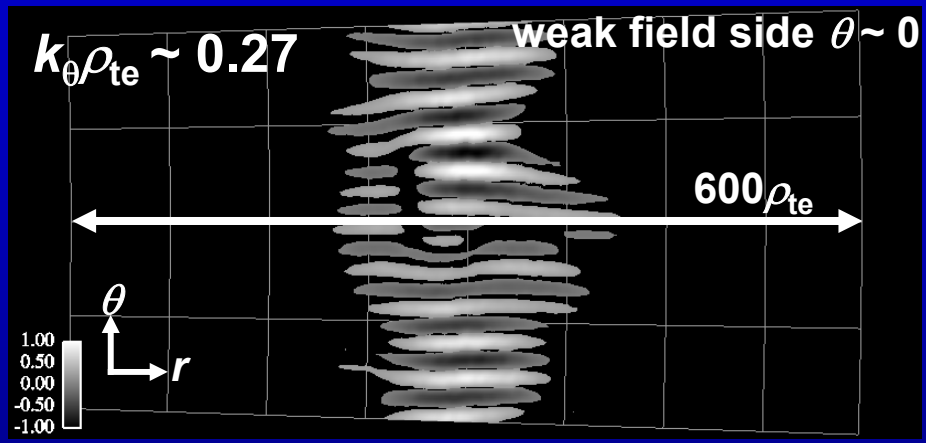

- QL streamers ($t\, v_{te}/L_n$ ~175)

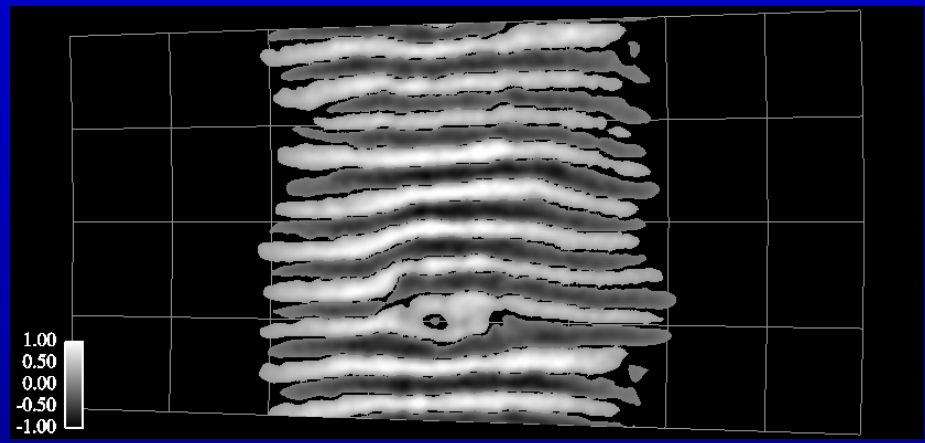

- Saturation phase ($t\, v_{te}/L_n$ ~208)

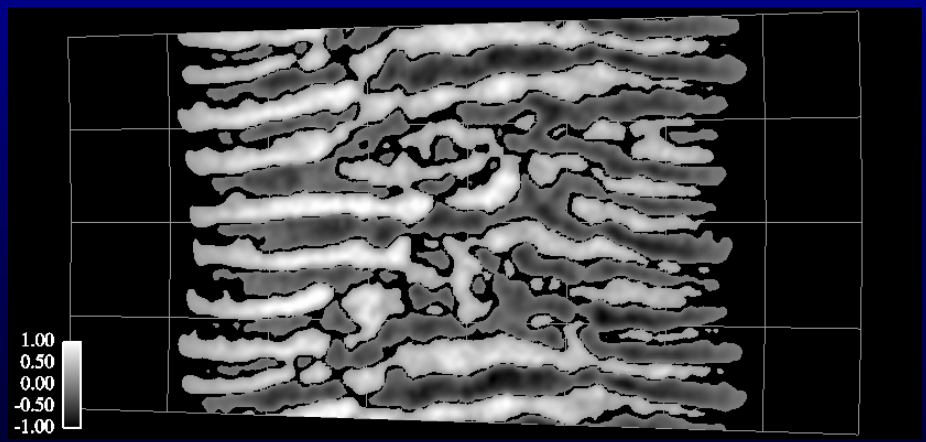

- Nonlinear streamers ($t\, v_{te}/L_n$ ~250)

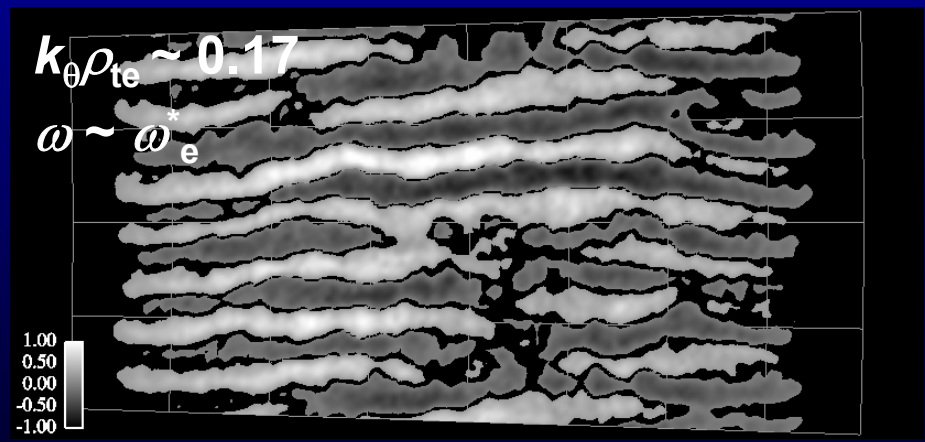

- PS-ETG turbulence is dominated by streamers
- Streamers are characterized by ballooning structure and $\omega \sim \omega^*_e$

Extremely high χ_e in PS-ETG turbulence

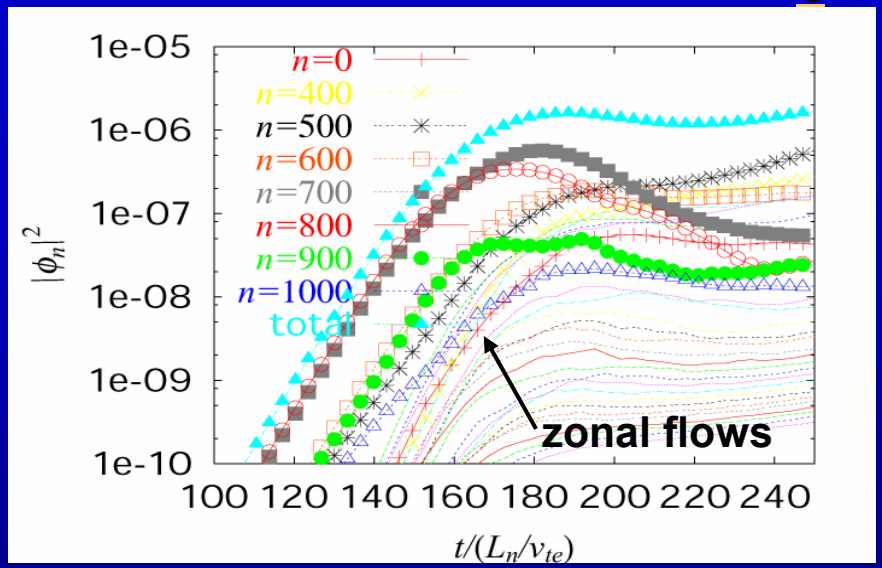

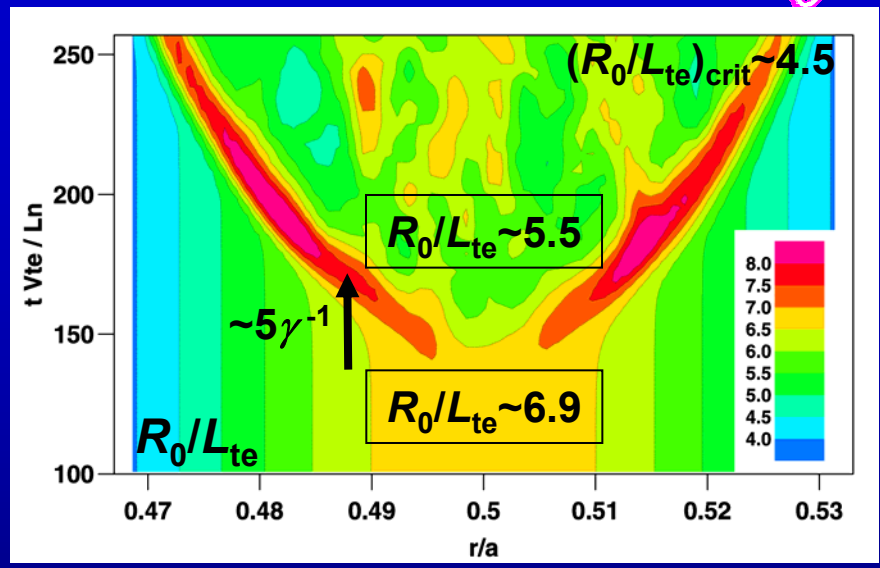

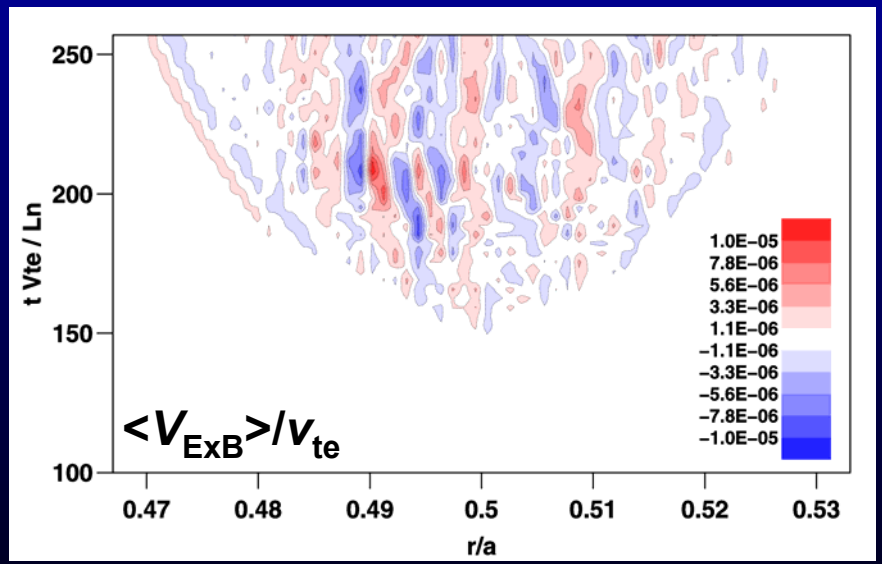

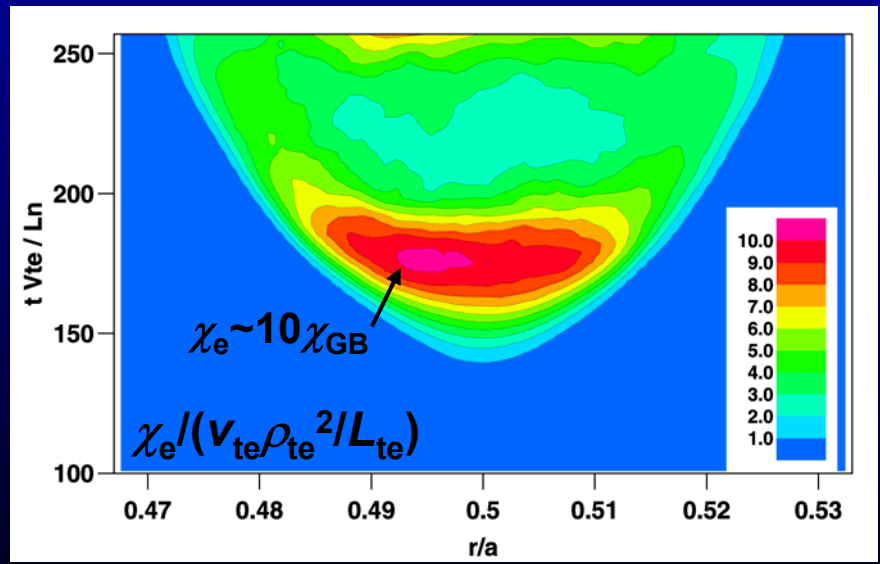

T_e profile is strongly relaxed in a turbulent time scale ~5γ^{-1}

Convergence of saturation levels against wedge size

- Time history of fluctuation field energy

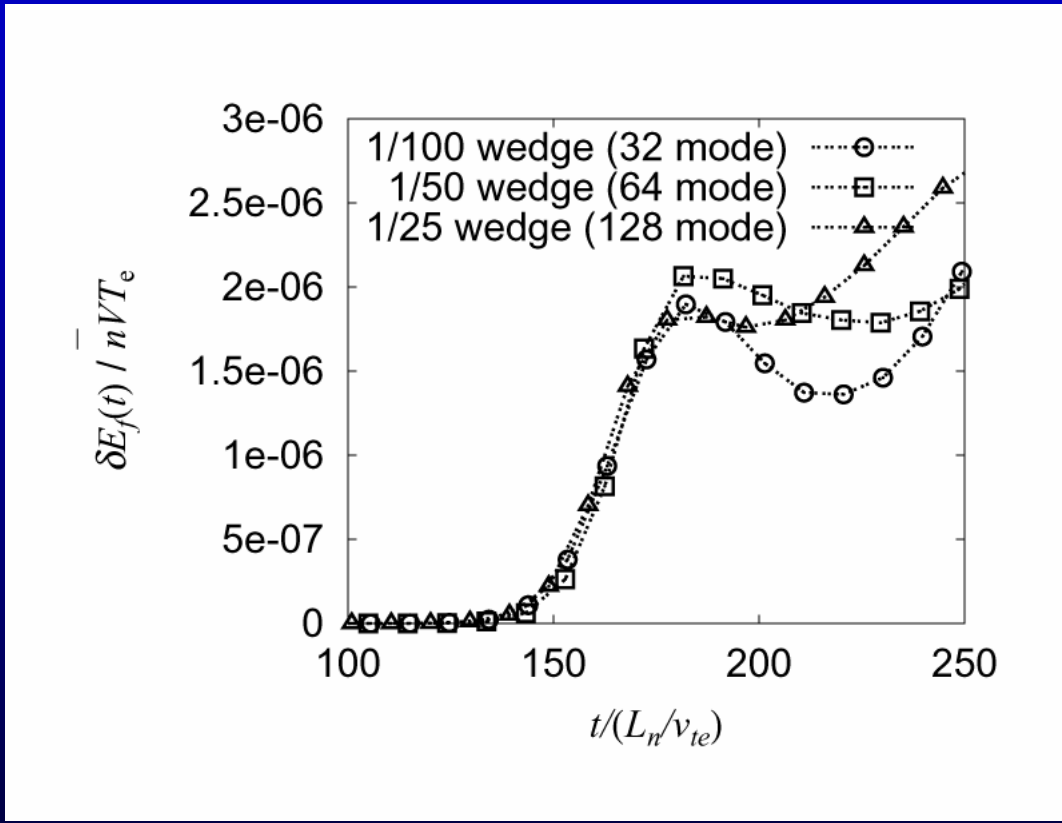

  - Saturation amplitude is converged against wedge torus size
  - Does nonlinear toroidal mode coupling (Lin 2004) lower saturation level?

Convergence of *n*-spectrum against wedge size

- 1/100 wedge torus, 32 mode
- 1/25 wedge torus, 128 mode

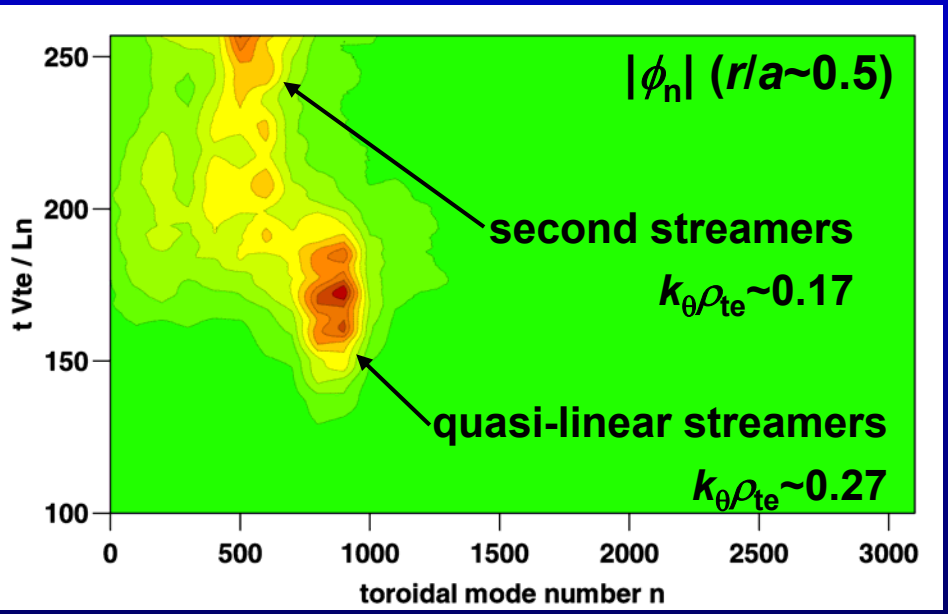

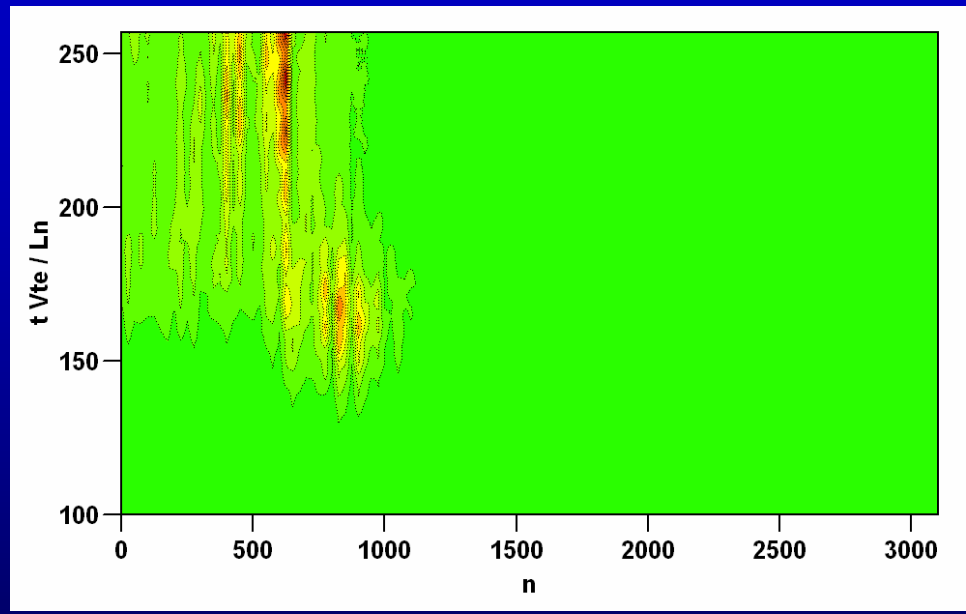

- Nonlinear spectrum is converged to coherent streamer mode
- QL streamers are excited at linearly most unstable $k_\theta\rho_{te}$
- 2nd streamers have coherent structure with $k_\theta\rho_{te}$~0.2
- Zonal flow component is very small

Zonal flow formation in RS-ETG turbulence

- Linear phase ($t\ v_{te}/L_n$ ~110)

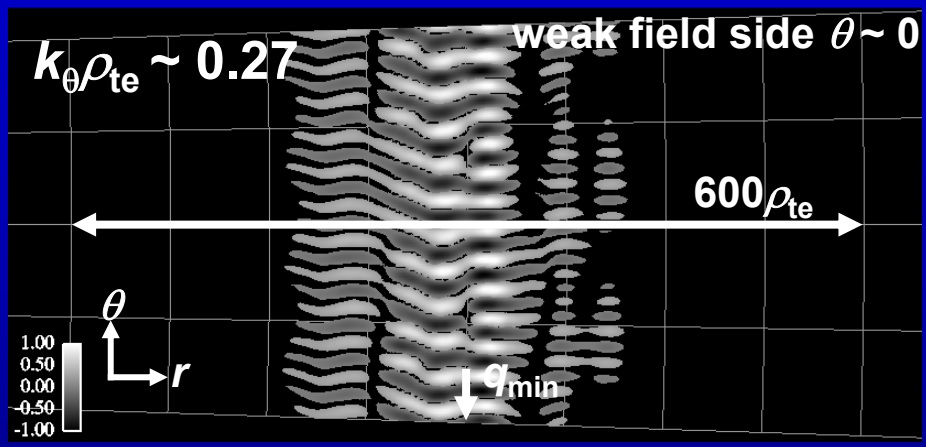

- Saturation phase ($t\ v_{te}/L_n$ ~207)

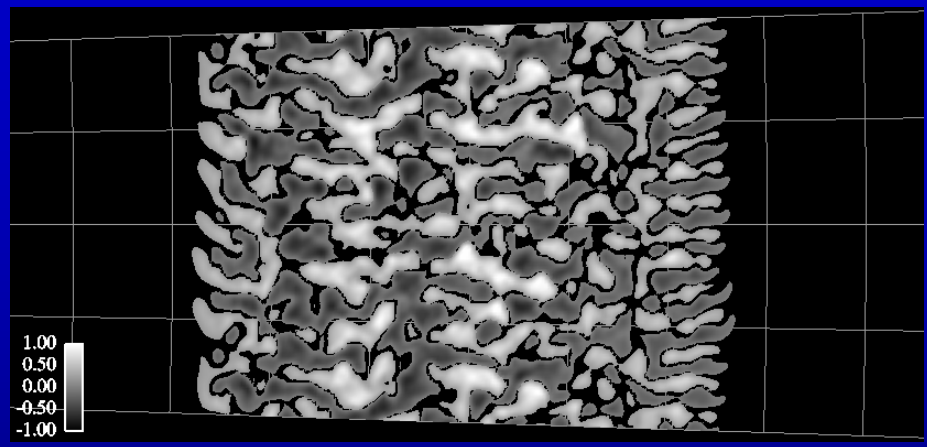

- Secondary mode ($t\ v_{te}/L_n$ ~255)

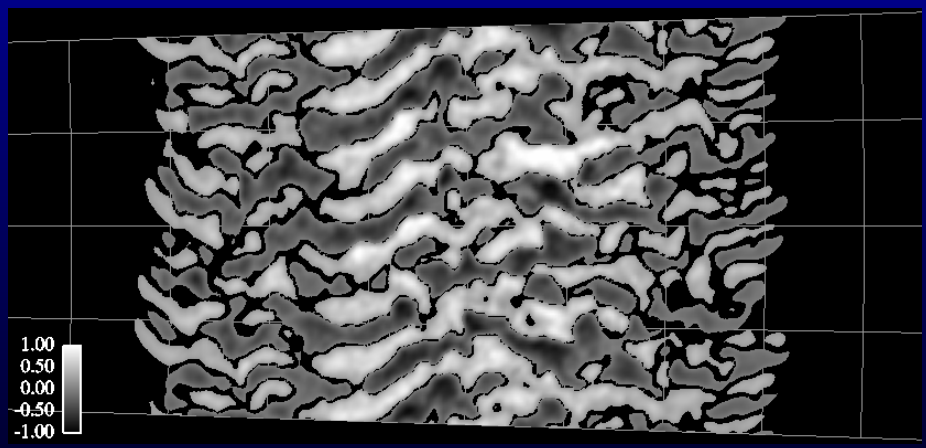

- Zonal flow formation ($t\ v_{te}/L_n$ ~380)

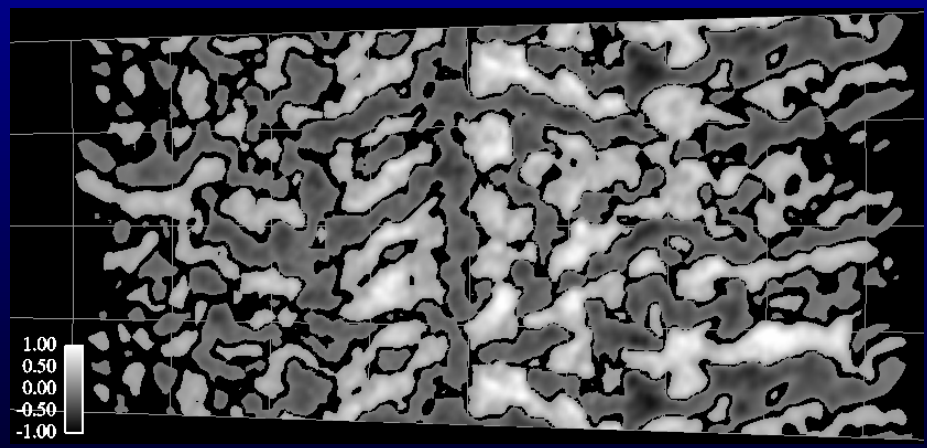

  - RS-ETG turbulence show qualitatively different behavior across q_{min}
  - Zonal flows (streamers) appear in negative (positive) shear region

χ_e gap structure in RS-ETG turbulence

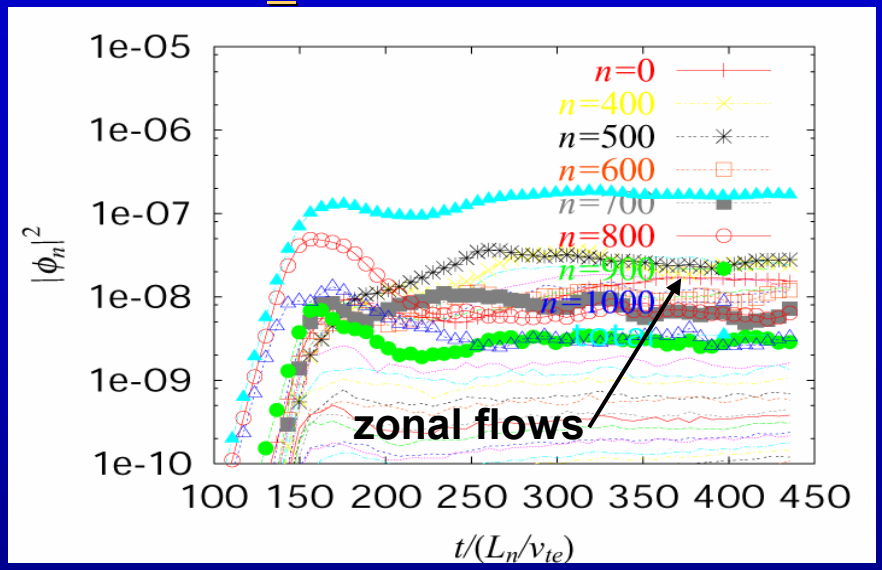

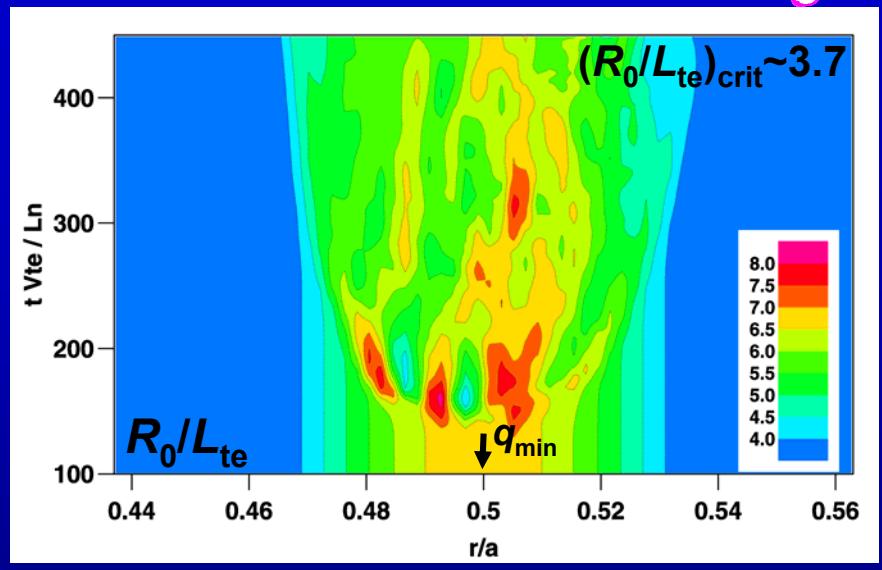

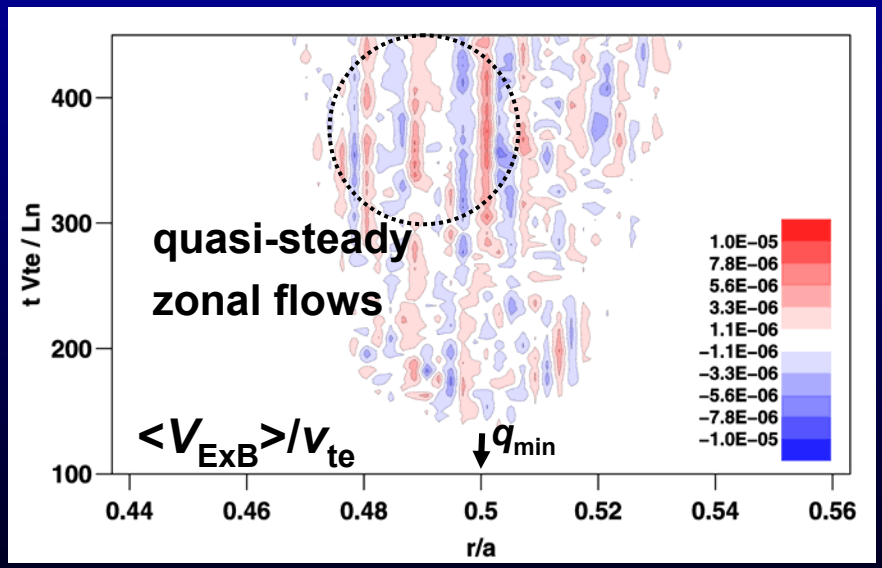

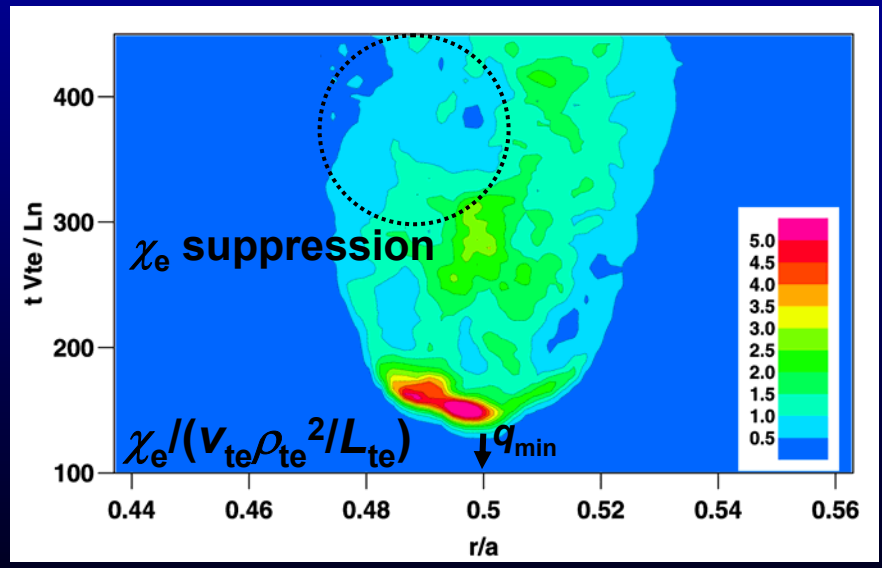

T_e gradient is sustained above its critical value in quasi-steady state

Summary(1)

- ETG turbulence is studied using global toroidal GK simulations
- Initial saturation levels consistent with the mixing length theory
  - Ballooning PS-ETG modes show Bohm like ρ^*-scaling
  - Slab like RS-ETG modes show gyro-Bohm like ρ^*-scaling
  - Small ρ^* PS-ETG modes give an order of magnitude higher saturation level than RS-ETG and large ρ^* PS-ETG modes
- PS/RS ETG turbulences show different structure formations
  - PS-ETG turbulence is dominated by streamers
    - T_e profile is quickly relaxed by large $\chi_e \sim 10 \chi_{GB}$
  - RS-ETG turbulence is characterized by zonal flows (streamers) in negative (positive) shear region
    - T_e profile is sustained by χ_e gap structure
- These results suggest a stiffness of T_e profile in PS tokamaks, and a possibility of the T_e transport barrier in RS tokamaks

Self-organization in ETG turbulence

Motivation to study self-organization of ETG-ZF

- ZFs are common phenomena not only in drift wave turbulence but also in Rossby wave turbulence
- While ZFs in Rossby wave turbulence are formed by self-organization (Williams 1978), ITG-ZFs are generated by modulational instability (Chen 2000)
  →Absence of adiabatic electron response to ITG-ZFs enhances modulational instability (Li 2002)
- In contrast, because of adiabatic ion response to ETG-ZFs, modulational instability is weak in ETG turbulence, and its governing equation is almost the same as Rossby wave turbulence
  →Does similar generation mechanism exist?
- To clarify generation mechanism of ETG-ZFs, self-organization process is studied in decaying electron turbulence simulations
  - Inverse energy cascade
  - Rhines scale length


ZF on planets

different? ⇕ same?

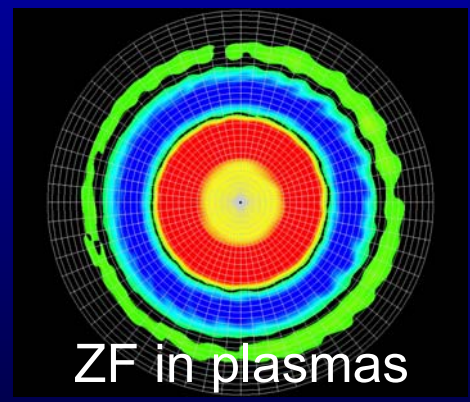
ZF in plasmas

Rhines scale length in Hasegawa-Mima Eq.

- In the limit of $k_{//} \to 0$, slab GK equations reduce to HM equation

$$\frac{\partial}{\partial t}\left(\rho_s^2 \nabla_\perp^2 \phi - \tau\phi\right) + \mathbf{b} \times \nabla_\perp \phi \cdot \nabla_\perp \left(\rho_s^2 \nabla_\perp^2 \phi + \ln n_0\right) = 0$$

$$\rho_s^2 = 1 + \lambda_{De}^2 / \rho_{te}^2, \quad \tau = T_e / T_i$$

- Conservation of energy E and potential enstrophy W

$$E = \frac{1}{2}\int \phi^2 + (\nabla_\perp \phi)^2 dV, \quad W = \frac{1}{2}\int (\nabla_\perp^2 \phi)^2 + (\nabla_\perp \phi)^2 dV$$

  - Turbulent binomial cascade (Hasegawa 1978)

  →Inverse energy cascade

  c.f. Selective dissipation of W (Kraichnan 1967)

- k_r regimes with wave like (linear term) and turbulent (nonlinear term) features are separated by Rhines scale length (Rhines 1975)

$$k_\beta \rho_s = (\beta / 2U)^{1/2} = 2^{-3/4} L_n^{-1/2} \varepsilon^{-1/4}$$

$$\beta = \nabla_\perp \ln n_0 = L_n^{-1}, \quad U = (2\varepsilon)^{1/2}, \quad \varepsilon = \frac{1}{2}\int (\nabla_\perp \phi)^2 dV$$

Decaying electron turbulence simulations

- Electrostatic GK slab PIC code (2.5D)
- Gyrokinetic electrons with adiabatic ions ($k_\perp \rho_{ti} >> 1$)
- Single helicity shear less slab model for q_{min} region
  - coordinate system (x,y,z) $\nabla_\perp \ln n_0 = L_n^{-1} \nabla x, \quad \mathbf{B} = B_0 \nabla z + B_1 \nabla y$
  - fixed ($\phi = 0$) and periodic boundary conditions in x and y
  - system size L_y = 292 ρ_{te}, L_x = 2 ~ 8L_y
  - $k_{//} = B_1/|\mathbf{B}| k_y = 8 \times 10^{-5} k_y$ (k_z=0)

  → E and W decay by Landau damping
- Plasma parameters
  - $\rho_{te}^2/\lambda_{De}^2 \sim 0.1$, $\tau \sim 0.3$
  - $L_n = 183\rho_{te} \sim \infty$, $L_{te} = \infty$
- Initial condition
  - sub-grid random noise
  - $e\phi/T_e \sim 0.005$

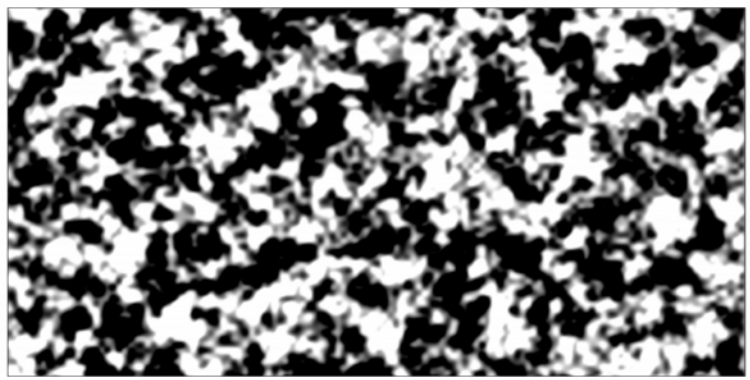

Contour plot of ϕ at t = 0

Turbulent structure is changed by density gradient

Contour plot of ϕ in quasi-steady relaxed state ($t\Omega_i$ = 870)

- $L_n=\infty$

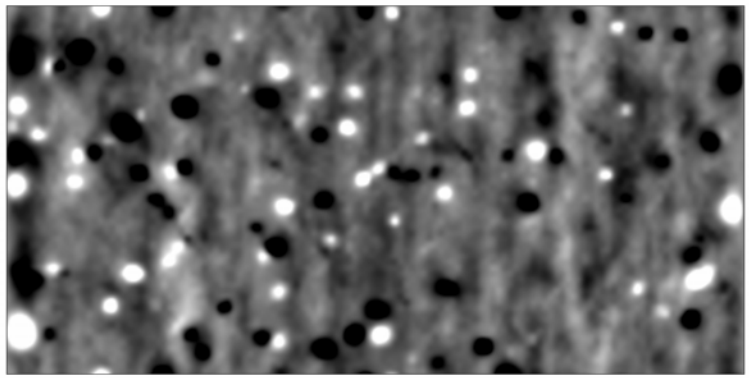

- Coherent isotropic vortices are produced
- Merger of like-sign vortices and decrease of vortices

→c.f. 2D fluid turbulence (McWilliams 1984)

- $L_n=1462\rho_{te}$

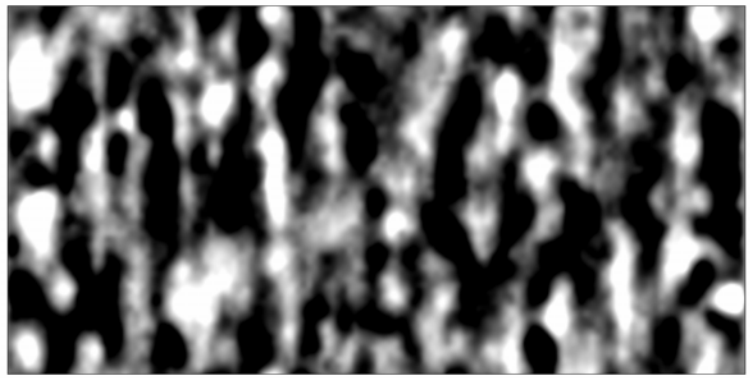

※$L_x=2L_y=584\rho_{te}$

- Anisotropic turbulent structure with zonal flows
- Zonal flows are produced by self-organization

Inverse energy cascade in self-organization

Decaying electron turbulence simulation with $L_n=731\rho_{te}$

- Time history of *E* and *W*
- Time history of $\bar{k}_x = \int k_x E_{k_x} dk_x \Big/ \int E_{k_x} dk_x$

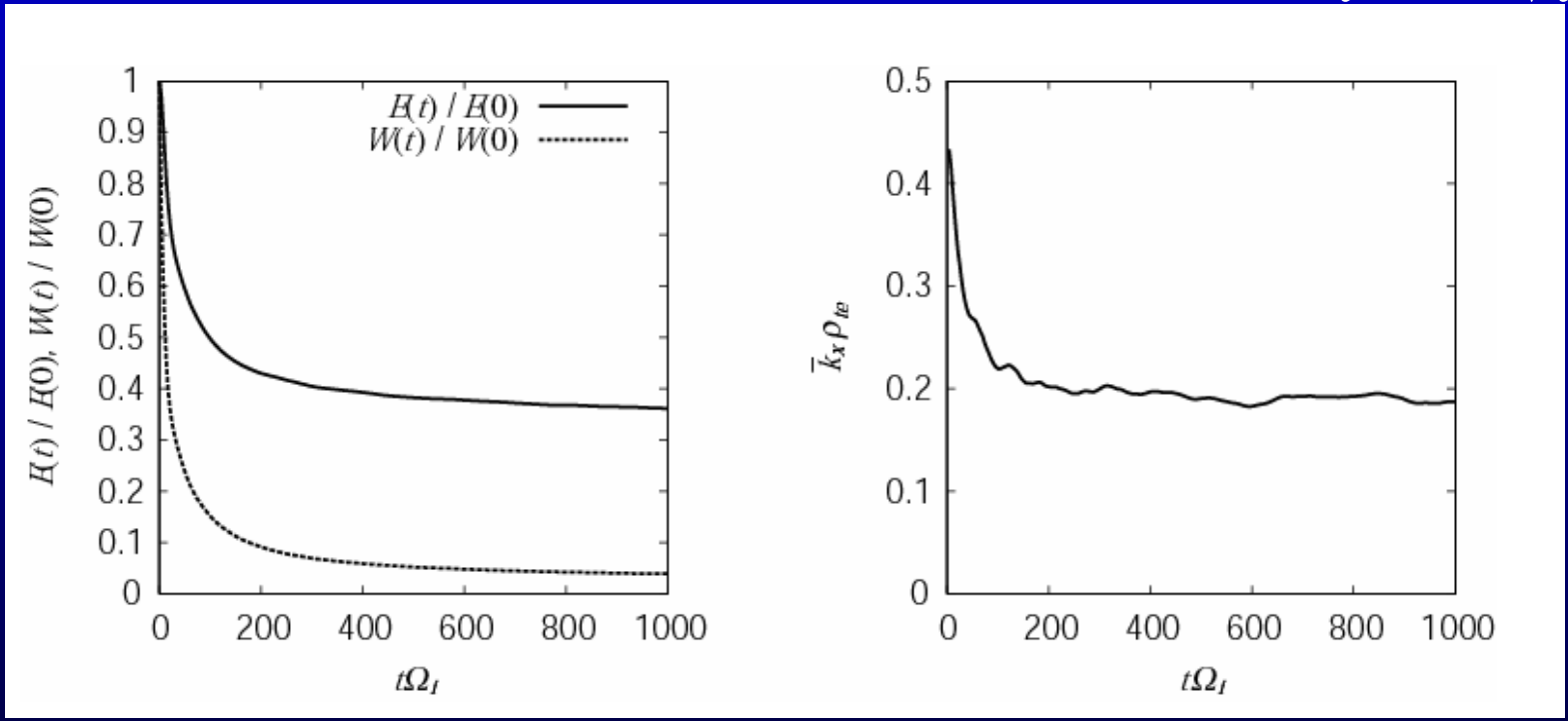

※ $L_x=8L_y=2336\rho_{te}$

- *W* decays much faster than *E*
- Average zonal flow wave number shifts to upscale in time

Rhines scale length in electron turbulence

- Summary of E, W and $\bar{k}_x$ values observed at $t\Omega_i = 1000$

L_n/ρ_{te}	$E(t)/E(0)$	$W(t)/W(0)$	$\bar{k}_x \rho_{te}$
1462	0.079	0.012	0.178
731	0.362	0.039	0.188
366	0.634	0.087	0.240
183	0.761	0.136	0.301

- Scaling of L_n, ε and $\bar{k}_x$

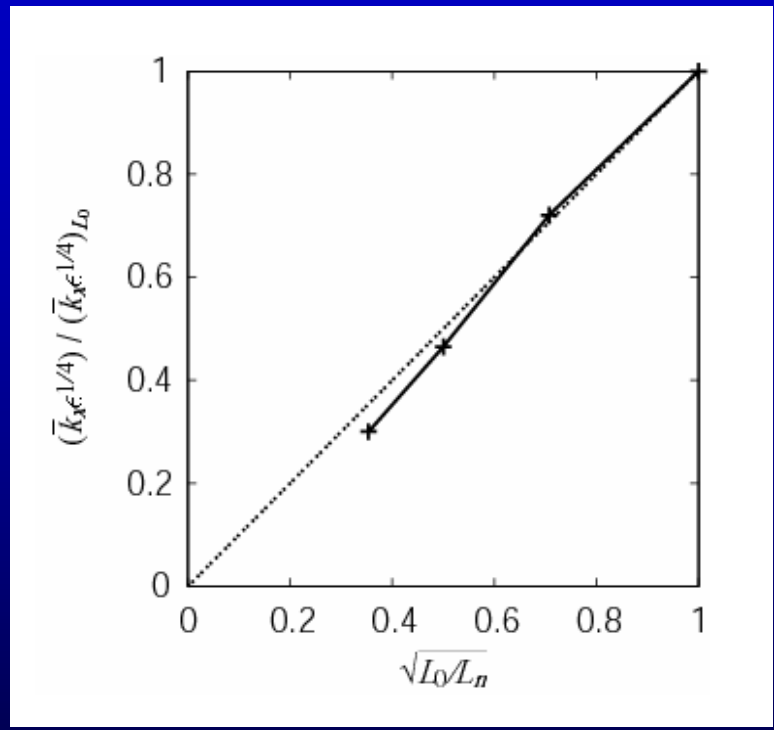

- Larger L_n^{-1} or $\omega^*/k_{//}$ leads to fluid limit (small dissipation)
- $\bar{k}_x$ becomes larger as L_n^{-1} increases
- Scaling $\bar{k}_x \propto L_n^{-1/2}\varepsilon^{-1/4}$ is consistent with Rhines scale length

Role of density gradient in ETG turbulence

ETG turbulence simulations with $\eta_e = L_n/L_{te} = \infty$ and $\eta_e = 5$

- $\eta_e = \infty$ (linear phase)

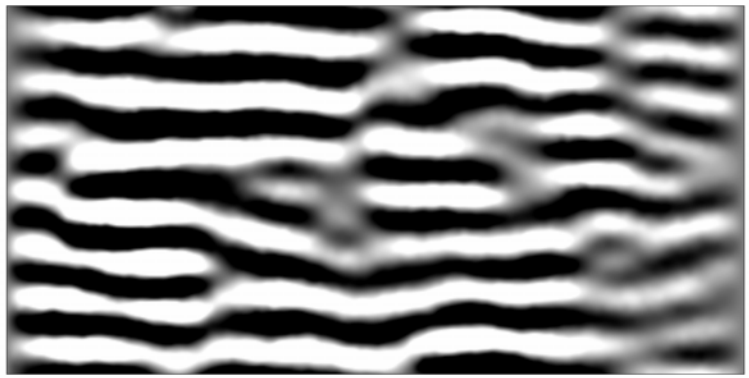

- $\eta_e = 5$ (linear phase)

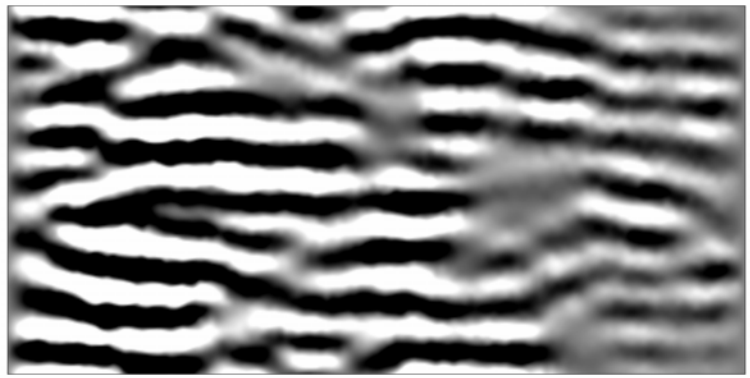

- $\eta_e = \infty$ (quasi-steady phase)

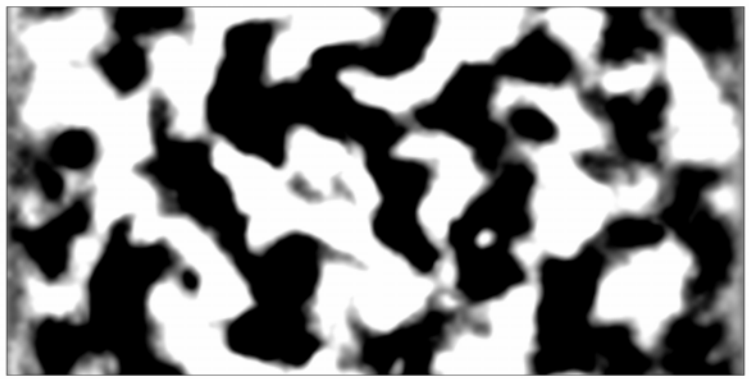

- $\eta_e = 5$ (quasi-steady phase)

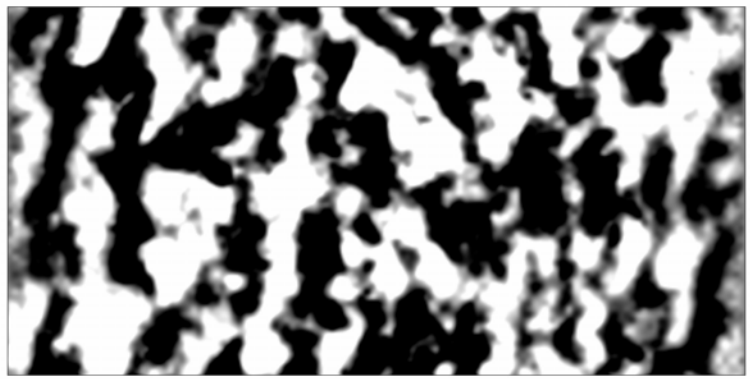

χ_e and ETG zonal flows can be controled by L_n

- Time history of χ_e in ETG turbulence with $\eta_e=\infty$ and $\eta_e=5$

※ L_{te} is chosen so that the same linear growth rates are given.

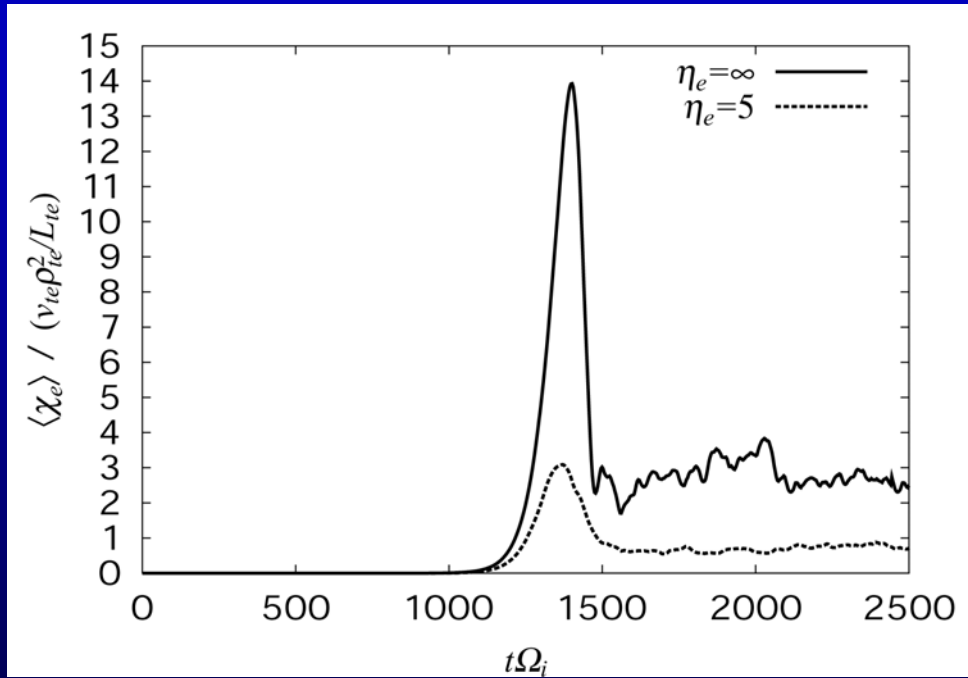

- Initial and quasi-steady saturation levels are χ_e~$14\chi_{GB}$ (χ_e~$3\chi_{GB}$) and χ_e~$3\chi_{GB}$ (χ_e~$0.7\chi_{GB}$) with $\eta_e=\infty$ ($\eta_e=5$)
- χ_e is enhanced more than 4 times by flat density profile.

Summary (2)

- Generation mechanism of ETG-ZFs is studied using decaying electron turbulence simulations
- ETG-ZFs are produced by self-organization processes
  - Inverse energy cascade is observed
  - ZF wave number is determined by Rhines scale length

  →ETG-ZFs can be controlled by density gradient
- Controllability of ETG-ZF is tested in ETG turbulence simulations with and without density gradient
  - Isotropic (anisotropic) turbulent structure is produced without (with) density gradient
  - χ_e is enhanced more than 4 times by flat density profile
- Slab ETG model may explain χ_e in tokamak core region where toroidal ETG mode and trapped electron mode are weak